

Dear Dr. Marc Salzmann, Topical editor,

Thank you very much for your feedback regarding our manuscript entitled “Comparative Analysis of MODIS, MISR, and AERONET Climatology over the Middle East and North Africa”. We greatly appreciate your comments. We have addressed all your comments and revised the manuscript accordingly.

Please find below a point-by-point response to your comments.

For your consideration, we have included a copy of the revised article with track changes.

Kindly let me know if I can provide more details regarding the manuscript.

Thank you,

Ashraf Farahat

Reviewers' comment

l. 95 to measures -> measures

Response

Done

Reviewers' comment

l. 110: Terra's -> Terra

Response

Done (now l.111 p5)

Reviewers' comment

l. 117 provides -> provide

Response

Done (now l.118 p5)

Reviewers' comment

l. 120 designed aerosol -> designed for aerosol

Response

Done (now l. 126 p5)

Reviewers' comment

l. 125 for (C005) ->? Please clarify

Response

l.131 p5: (C005) modified to Collection 5 (C005),
also l.129 p5 Level 2 (C006) modified to Level 2 – Collection 6 (C006)

Reviewers' comment

l. 126: land respectively -> land, respectively.

Response

Done (now l. 136 p6)

Reviewers' comment

l. 197: A good aspect -> An advantage

Response

Done (now l. 126 p9)

Reviewers' comment

l. 211: less error -> smaller deviations from the AERONET data

Response

Done (now l. 228 p9)

Reviewers' comment

l. 226f: either "than those" -> "than that" or else: "daily variability ... s" -> "daily variabilities ... are"

Response

Done "than those" -> "than that" (now l. 246 p10)

Reviewers' comment

l. 227: at -> in

Response

Done (now l. 246 p10)

Reviewers' comment

l. 264 and also in lines 267, 436, and 808: Long-range -> Long-term

Response

Done

Reviewers' comment

l. 275: omit "of"

Response

Done (now l. 299 p12)

Reviewers' comment

l. 289: illustrated -> shown

Response

Done (now l. 313 p12)

Reviewers' comment

l. 318: capture -> captures

Response

Done (now l. 344 p14)

Reviewers' comment

l. 379: present -> represent

Response

Done (now l.390 p 16)

Reviewers' comment

l. 425: Can -> Can be

Response

Done (now l.436 p 18)

Reviewers' comment

l. 425: atmosphere -> the atmosphere

Response

Done (now l.436 p 18)

Reviewers' comment

l. 479: while show -> while they show

Response

Done (now l.481 p 20)

Reviewers' comment

l. 480: do a good job -> perform well

Response

Done (now l.491 p20)

Reviewers' comment

l. 481: present -> represent

Response

Done (now l.508 p20)

Reviewers' comment

The following point regarding MODIS from the author's response should be clarified in the materials and methods section:

Both dark target and deep blue algorithms have been used. Dark target retrievals were used over water regions while deep blue data were used over land. For regions like Bahrain where large water body surrounds land, a combined Dark Target and Deep Blue AOD for land and Ocean has been used.

Response

Lines 121-125 P5 have been added to the manuscript

The Deep Blue (DB) is a NASA developed algorithm to calculate AOD over land using MODIS data. By measuring contrast between aerosols and surface features, DB retrieves AOD. Over bright land, DB uses (0.412, 0.470/0.479 μm) for AOD retrievals. Over water, the DB algorithm is not used, but the Dark Target (DT) algorithm is used instead.

Lines 138-144 P6 have been also added to the manuscript

Both DB and DT algorithms have been used in this study. DB data were used over land, while DT retrievals were used over water. For regions like Bahrain where large water body surrounds land, a combined DB and DT algorithm for land and ocean has been used. This is because the MODIS matched ground-based AERONET station in Bahrain (described in section 2.3 and Table 1) is located less than 2 km from the coastline. This makes MODIS combine retrievals for both land and water over this station. Data are available at <https://giovanni.gsfc.nasa.gov/giovanni>.

Reviewers' comment

As far as I can see, the last point raised by reviewer #1 was not answered. Table 1 says that AERONET data for Cairo is available for 2005 -2007, but this is inconsistent with Fig. 4b and the newly added text. Is the data displayed in Figure 3b available from the AERONET website? Please re-check!

Response

I agree with the reviewer's comment and I am very sorry, as I have overlooked that comment in my last response. There are two main sets of AERONET data available over Cairo; namely Cairo

EMA and Cairo EMA_2. Data listed under Cairo EMA are available from 2005 – 2007 only, while data listed under Cairo EMA_2 are available from 2010 – 2017.

In this study, we are comparing satellites' retrievals with AERONET station data using measurement that are within a radius of ~ 27.5 km from the AERONET station and about 30 min of each satellite flyover the AERONET location. For the Cairo station, we have these satellite matching data available for the Cairo EMA_2 retrievals; that is why we have used these data in Figure 4b.

We have now modified table 1 for Cairo AERONET station to show that the data available are from 2010-2017, which now matches figure 4b.

All AERONET data are available through <https://aeronet.gsfc.nasa.gov>

More details: to download data for the Cairo AERONET station

- Visit <https://aeronet.gsfc.nasa.gov>
- Under AEROSOL OPTICAL DEPTH (V3) click on Download Tool.
- Under Geographic Location pick “North_Africa” then click on “Get Country or State”
- Pick Egypt then click on Get AERONET Sites and pick Cairo_EMA_2.
- Click on Get Download Form.
- Data are available until 26-04-2010 to 14-03-2017

Note: AERONET satellite matching data are available by request through Jet Propulsion Laboratory (JPL)/NASA.

1 **Comparative Analysis of MODIS, MISR and AERONET Climatology**
2 **over the Middle East and North Africa**

3 **Ashraf Farahat**

4 Department of Physics, King Fahd University of Petroleum and Minerals, Dhahran 31261,
5 Saudi Arabia;
6 E-Mails: farahata@kfupm.edu.sa

7 *Author to whom correspondence should be addressed; E-Mail: farahata@kfupm.edu.sa.

8 Tel: (321) 541-7088

9
10 **Abstract:**

11 Comparative analysis of MISR MODIS, and AERONET AOD products is performed
12 over seven AERONET stations located in the Middle East and North Africa for the
13 period of 2000 – 2015. Sites are categorized into dust, biomass burning and mixed.
14 MISR and MODIS AOD agree during high dust seasons but MODIS tends to
15 underestimate AOD during low dust seasons. Over dust dominated sites, MODIS/Terra
16 AOD indicate a negative trend over the time series, while MODIS/Aqua, MISR, and
17 AERONET depict a positive trend. A deviation between MODIS/Aqua and
18 MODIS/Terra was observed regardless of the geographic location and data sampling.
19 The performance of MODIS is similar over the entire region with ~64 percent of AOD
20 within the $\Delta\tau = \pm 0.05 \pm 0.15\tau_{AERO}$ confidence range. MISR AOD retrievals fall within
21 84 percent of the same confidence range for all sites examined here. Both MISR and
22 MODIS capture aerosol climatology; however few cases were observed where one of
23 the two sensors better captures the climatology over a certain location or AOD range
24 than the other sensor. AERONET Level 2.0 Version 3, MODIS Collection 6.1, and
25 MISR V23 data have been used in analyzing the results presented in this study

26 **Keywords:** AOD; Remote Sensing; North Africa; Middle East; Validation

27
28
29
30

31 **1. Introduction**

32 The Middle East and North Africa host the largest dust source in the world, the Sahara Desert
33 in North Africa that may be responsible for up to 18 percent of global dust emission (Todd
34 et al., 2007, Bou Karam et al. 2010, Schepanski et al. 2016). The vast 650,000 km² Rub' al
35 Khali (Empty Quarter) sand desert is a major source of frequent dust outbreaks and severe
36 dust storms that has major effect on human activity in the Arabian Peninsula (Böer, 1997,
37 Elagib and Addin 1997, Farahat et al., 2015).

38 Air quality over the Arabian Peninsula has received significant attention during the past 15
39 years due to unprecedented overall economic growth, and a booming oil and gas industry,
40 however, air pollution studies are still far from complete. Frequently blowing dust storms
41 play a significant role in pollutant transport over the Arabian Peninsula; and major
42 environmental pollution events such as burning of Kuwait oil fields during the 1991, Gulf
43 War resulted in a large environmental impact on the Arabian Gulf Area (Sadiq and McCain,
44 1993, and Farahat 2016).

45 Aerosol optical depth, AOD, (also called aerosol optical thickness, AOT) as a parameter
46 indicates the extinction of a beam of radiation as it passes through a layer of atmosphere that
47 contains aerosols. Both satellites and ground-based instruments can be used to measure AOD
48 in the atmosphere, but within the same temporal coordinates and geographic location
49 different instruments could generate different retrievals (Kahn et al., 2007, Kokhanovsky et
50 al., 2007, Liu et al., 2008 and Mishchenko et al., 2009).

51 Since the turn of the 21st century, an upward trend of remotely sensed and ground-based
52 AOD and air pollutants was observed over the Middle East and North Africa (El-Askary
53 2009, Ansmann et al. 2011, Yu et al. 2013, Chin et al. 2014, Yu et al. 2015, Farahat et al.
54 2016, Solomos et al. 2017). This positive trend is attributed to the increase in the Middle
55 Eastern dust activity (Hsu et al., 2012) due to changes in wind speed and soil moisture
56 (Ginoux et al. 2001 and Kim et al. 2013). Yu et al., (2015) concluded that the persistent La

Formatted: Font: Not Italic, Complex Script Font: Not Italic

57 Niña conditions (Hoell et al., 2013) have caused increment in Saudi Arabian dust activity
58 during 2008 – 2012. Energy subsidies also encourages energy overconsumption in the
59 Middle East and North Africa with little incentive to adopt cleaner technology. Lack of
60 applying strict environmental regulations have permitted exacerbated urban air pollution.
61 During the last two decades, a large number of satellites, ground stations and computational
62 models contributed to build global and regional maps for the temporal and spatial aerosol
63 distributions. While, ground-based stations and field measurements can identify aerosols
64 properties over specific geographic locations, the sparse and non-continues data from ground-
65 based sensors scattered over the Middle East and North Africa is not sufficient to provide
66 information on spatial and temporal trends of particulate pollution. On the other hand,
67 satellites imagery could provide a significant source of data mapping over larger areas.
68 For its wide spatial and temporal data availability space-born sensors are important sources
69 to understand aerosols characteristics and transport, however low sensitivity to particle type
70 under some physical conditions, high surface reflectivity, persistent cloud, and generally low
71 aerosol optical depth could limit satellite data application in characterizing properties of
72 airborne particles, especially in the Middle East.

73 In order to evaluate the efficiency of space-borne sensors in representing ground observations
74 recorded by AERONET stations we have performed detailed statistical inter-comparison analysis
75 between satellite AOD products and AERONET for seven stations in the Middle East and North
76 Africa representative for dust, biomass burning, and mixed aerosol conditions (Dubovik et al.,
77 (2000, 2002, 2006), Holben et al. (2001), Derimian et al., (2006), Basart et al. (2009), Eck
78 el. (2010), Marey et al., 2010, Abdi et al., (2012)). Previously we analysed these seven
79 AERONET stations to understand particles categorization and absorption properties (Farahat
80 et al. 2016), and the current study extends the analysis to the satellite datasets.

81 In the first part of this article, we validated MISR and MODIS retrievals against collocated
82 AERONET observations. We also assessed the consistency in aerosol trends between space-
83 borne sensors and ground-based data.

84 In the second part, we evaluated representativeness of satellite-derived aerosol climatology
85 over the study region from the long-term AERONET data for MISR and MODIS AOD
86 products. It is especially relevant for the MISR instrument, as its sampling is limited by once
87 per week observations of the same region from the two overlapping paths. MODIS provides
88 nearly daily observations to the same geographic location; however, the quality of the product
89 diminishes over the bright targets potentially affecting MODIS-derived aerosol climatology.
90 The collocated MISR, MODIS and AERONET data were obtained at the MAPSS website
91 (<http://giovanni.gsfc.nasa.gov/mapss.html>).

92

93 **2. Materials and Methods**

94 **2.1 MISR**

95 The Multi-angle Imaging SpectroRadiometer (MISR) instrument to measure tropospheric
96 aerosol characteristics through the acquisition of global multi-angle imagery on the daylight
97 side of Earth. MISR applies nine Charge Coupled Devices (CCDs), each with 4 independent
98 line arrays positioned at nine view angles spread out at nadir, 26.1°, 45.6°, 60.0°, and 70.5°.
99 In each of the nine MISR cameras, images are obtained from reflected and scattered sunlight
100 in 4 bands blue, green, red, and near-infrared with a centre wavelength value of 446, 558,
101 672, and 867 nm respectively. The combination of viewing cameras and spectral wavelengths
102 enables MISR to retrieve aerosols AOD over high reflection surfaces like deserts.

103 In this study, we use Level 2 (ver. 0023) AOD at 558 nm (green band) measured by MISR
104 instrument with a 17.6 km resolution aboard the Terra satellite. MISR Level 2 aerosol
105 retrievals use only data that pass angle-to-angle smoothness and spatial correlation tests

Deleted: s

107 (Martonchik et al. 2002), as well as stereoscopically derived cloud masks and adaptive cloud-
108 screening brightness thresholds (Zhao and Di Girolamo, 2004).

Deleted:

Formatted: Font: (Default) Times New Roman, Complex
Script Font: Times New Roman

109 2.2 MODIS

110 The Moderate Resolution Imaging Spectroradiometer (MODIS) is a payload instrument on
111 board the Terra and Aqua satellites. Terra and Aqua orbit around the Earth from North to
112 South and South to North across the equator during the morning and afternoon respectively
113 (Kaufman et al., 1997). Terra MODIS and Aqua MODIS provides nearly daily coverage of
114 the Earth's surface and atmosphere in 36 wavelength bands, ranging from 0.412 to 41.2 μm ,
115 with spatial resolutions of 250 m (bands 1-2), 500 m (bands 3-7), 1000 m (bands 8-36).
116 Located near-polar orbit (705 km), MODIS has swath dimensions of 2330 km \times 10 km and
117 a scan rate of 20.3 rpm. With its high radiometric sensitivity and swath resolution MODIS
118 retrievals provide information about aerosols optical and physical characteristics. MODIS
119 uses 14 spectral band radiance values to evaluate atmospheric contamination and determine
120 whether scenes are affected by cloud shadow (Ackerman et al., 1998).

Deleted: s

121 The Deep Blue (DB) is a NASA developed algorithm to calculate AOD over land using
122 MODIS data. By measuring contrast between aerosols and surface features, DB retrieves
123 AOD. Over bright land, Deep Blue uses (0.412, 0.470/0.479 μm) for AOD retrievals. Over
124 water, the DB algorithm is not used, but the Dark Target (DT) algorithm is used instead.

Deleted: s

125 The MODIS DT algorithm is designed for aerosol retrieval from MODIS observations, over
126 dark land surfaces (low values of surface reflectance) (e.g., dark soil and vegetated regions)
127 in parts of the visible (VIS, 0.47 and 0.65 μm) and shortwave infrared (SWIR, 2.1 μm)
128 spectrum (Kaufman et al., 1997). Level 2 – Collection 6 (C006) of the algorithm are used to
129 retrieve MODIS aerosols' time series data. Levy *et al.* (2010) reported that the dark-target
130 algorithm AOD at 550 nm measurement for Collection 5 (C005) includes uncertainty of \pm
131 $(0.05\tau+0.03)$ and $\pm (0.15\tau+0.05)$ over ocean and land, respectively. This uncertainty is

Deleted: dark-target

136 caused by uncertainties in computing cloud masking, surface reflectance, aerosol model type
137 (e.g., single scattering albedo), pixels selections and instrument calibration.

138 Both DB and DT algorithms have been used in this study. DB data were used over land,
139 while DT retrievals were used over water. For regions like Bahrain where large water body
140 surrounds land, a combined DB and DT algorithm for land and ocean has been used. This is
141 because the MODIS matched ground-based AERONET station in Bahrain (described in
142 section 2.3 and Table 1) is located less than 2 km from the coastline. This makes MODIS
143 combine retrievals for both land and water over this region. Data are available at
144 <https://giovanni.gsfc.nasa.gov/giovanni>.

145 **2.3 AERONET**

146 The Aerosol Robotic Network (AERONET) (Holben et al., 1998 and Holben et al., 2001) is
147 a ground-based remote sensing aerosols network that provides a long-term data related to
148 aerosol optical, microphysical and radiative properties. With over 700 global stations, the
149 AERONET data is widely used in validating satellite retrievals (Chu et al., 1998 and
150 Higurashi et al., 2000).

151 The sun photometers used by AERONET measure spectral direct-beam solar radiation, as
152 well as directional diffuse radiation in the solar almucantar. The former are used to determine
153 columnar spectral AOD and water vapour, provided at a temporal resolution of
154 approximately 10–15 min (Sayer et al. 2014). AERONET direct-sun AOD has a typical
155 uncertainty of 0.01–0.02 (Holben et al., 1998) and is provided at multiple wavelengths at
156 340, 380, 440, 500, 675, 950, and 1020 nm.

157 Seven AERONET sites were selected for satellite validation in this study (Table 1.). The sites
158 were selected based on their geographic locations to represent aerosols characteristics over
159 North Africa and the Middle East (Farahat et al., 2016). A record of long-term data collection
160 was another factor in the selection process.

161 **Data Matching Approach**

162 Multi-sensors data matching requires using only compatible data to eliminate uncertainties
163 associated with cloud shadow and spatial and temporal retrievals produced by different
164 instruments (Liu and Mishchenko (2008) and Mishchenko et al., 2009).

165 The comparison of MISR and MODIS products against AERONET is performed to evaluate
166 satellites' retrieval over individual North Africa and Middle East sites (see Table 1). There
167 is only a small number of AERONET measurements that are perfectly collocated with
168 MODIS and MISR. One way to work with this lack of compatibility problem is to compare
169 satellites measurements nearby a certain AERONET site and comparing AERONET
170 measurements nearly synchronized with the satellite overpass time (Sioris et al. 2017).

171 Another reasonable strategy is to average all satellite measurements with a certain distance
172 of an AERONET location and average all AERONET measurements within a certain time
173 range (Mishchenko et al., 2010). The results presented in this paper are based on the second
174 approach as it compares average spatial satellite measurements with average temporal
175 AERONET measurements. We implemented the Basart et al., (2009) approach in using a
176 spatial and temporal threshold of 50 km and 30 min for MISR, MODIS, and AERONET data
177 matching.

178 We use the Giovanni Multi-sensor Aerosol Products Sampling System MAPSS
179 (<http://giovanni.gsfc.nasa.gov/aerostat/>) for the data inter-comparison as aerosols products
180 are averaged from measurements that are within a radius of ~ 27.5 km from the AERONET
181 station and within 30 min of each satellite flyover over this location. These data are
182 represented in the article by MISR / MODIS “matched AERONET data”.

183 “All data” represents AOD products at the selected station. AERONET station ‘all data’
184 are obtained through AEROSOL ROBOTIC NETWORK (AERONET) website
185 (<https://aeronet.gsfc.nasa.gov/>). Daily AOD data with level 2.0 quality was used in the

186 analysis (Smirnov et al., 2000) . Level 2.0 AOD retrievals are accurate up to 0.02 for mid-
187 visible wavelengths.

188 MISR ‘all data’ is available through MISR website (<https://www.misr.jpl.nasa.gov>).

189

Formatted: Font color: Hyperlink

Deleted: -

Deleted: /getData/accessData/

190 3. Statistics

191 We have used two statistical parameters to compare data retrievals from space-borne and
192 ground based sensors including:

193 (1) Correlation coefficient (R),

194 The correlation coefficient is a parameter to measure data dependence. If the value of R is
195 close to zero, it indicates weak data agreement. And values close to 1 or -1 indicate that data
196 retrievals are positively or negatively linearly related (Cheng et al., 2012).

197

198 (2) Good Fraction (G- fraction).

199 The G- fraction indicator uses a data confidence range defined by MISR and MODIS
200 (Bruegge et al., 1998 and Remer et al., 2005) over the land and ocean that combines absolute
201 and relative criterion and weights data equally such that small abnormalities will not affect
202 the inter-comparison statistics (Kahn et al., 2009). In this study, we use MODIS confidence
203 range which defines data retrieval as “good” if the difference between MODIS and
204 AERONET is less than

$$205 \Delta\tau = \pm 0.03 \pm 0.05\tau_{AER}, \text{ Over ocean,} \quad (1)$$

$$206 \Delta\tau = \pm 0.05 \pm 0.15\tau_{AER}, \text{ Over land.} \quad (2)$$

207

208 where τ_{AER} is the optical depth retrieved using AERONET stations. The G-fraction is the
209 percentage of MODIS data retrievals that satisfies (Equations (1) and (2)) over ocean and

212 land respectively. Optical depth threshold over land (Equation (1)) is higher than over ocean
213 (Equation (2)) due to harder data retrievals and high data instability over land.

214 An advantage of using data confidence range is excluding small fraction data outliers from
215 producing inexplicably large influence on comparison statistics by weighting all events
216 equally.

Deleted: good aspect

217

218 4. Results and discussion

219 4.1 Validating MISR and MODIS AOD retrievals against AERONET observations 220 over the Middle East and North Africa

221 Illustrated in Figures 2, 3 and Tables 2, 3 is a regression analysis of MISR and MODIS Terra
222 AOD products against AERONET AOD over the seven AERONET sites, shown in Table1,
223 from 2000 – 2015.

224 The correlation coefficient between MISR and AERONET AOD at region 1 is equal to or
225 above 0.85 except in Bahrain during DJF and JJA (Figure (2) and Table 2), which could be
226 attributed to lack of data and the impact of water surface reflectivity over Bahrain. Similar
227 correlation coefficient values were found in region 2 where MISR-AERONET AOD shows

228 smaller deviations from the MODIS data (Figures (2, 3) and Table 3). In general, MODIS-
229 AERONET AOD correlation coefficient is lower than those of MISR at all sites, except
230 Mezaira, where MISR and MODIS matched AERONET AOD correlation almost match.

Deleted: less error than

231 The lowest MODIS-AERONET AOD correlation coefficient was found over Cairo but could
232 be attributed to the lack of data availability at this location (Figs 3e-h). Low values of
233 MODIS-AERONET correlation coefficient is also found over Saada, Taman, and Sedee
234 Boker sites.

235 Over all AERONET stations, the number of MODIS AERONET matched AOD are 4 to 8
236 times those of MISR which is expected from the MISR's sampling.

239 Comparisons show that the difference between MISR and MODIS retrievals at the selected
240 AERONET sites could be significant as expected from the MODIS ~~DT~~ algorithm
241 performance over bright land surfaces Kokhanovsky et al. (2007).

Deleted: Dark Target

242 High AOD values over regions 1 and 2 measured by both AERONET and satellites' sensors
243 indicate higher dust activities that peaks during May – Aug during dust storms season. Higher
244 AOD values recorded during SON over Cairo station could be caused by seasonal rice straw
245 burning by farmers in Cairo, an environmental phenomena known as Cairo Black cloud
246 (Marey et al. 2010). As shown in (Figure (3)), the daily variability in MODIS measurements
247 is larger than ~~that of MISR in~~ all the three regions. In general, MODIS tends to underestimate
248 the AOD values on low dust seasons (Figures (2, 3) and Tables 2, 3).

Deleted: those

Deleted: at

249 The MODIS underestimated AOD values are more noticeable over Bahrain. This could be
250 attributed to large water body surrounding Bahrain, which should affect surface reflectivity.
251 Moreover, water in the Arabian Gulf has been polluted in recent years (Afnan 2013), leading
252 to possible changes in watercolour and uncertainties in calculating surface reflectivity. The
253 patchy land surface or pixel grid contaminated by water body is the dominant error sources
254 for MODIS aerosol inversion over the land areas (He et al. 2010).

255 Compared to MODIS, MISR's outperform in retrieving AOD over region 1 including vast
256 highly reflecting desert areas can be attributed to its multispectral and multi-angular
257 coverage, which make MISR provide better viewing over a variety of landscapes.
258 Meanwhile, MISR retrieval also takes into consideration aerosols' particles nonsphericity,
259 which could have significant effect on its AOD retrievals (von Hoyningen-Huen and Posse
260 1997). MISR's retrieval did not perform well over Cairo site due to lack of matched points
261 in most of the seasons (15 in DJF, 39 in MAM, 61 in JJA, and 23 in SON during 2000 -
262 2015).

263

267 **4.2 Trends of AOD MISR, MODIS, and AERONET retrievals over the Middle East**
268 **and North Africa**

269 Figure 4 shows time series of monthly mean AOD derived from MODIS/Aqua,
270 MODIS/Terra, MISR and AERONET over a) dust b) biomass and c) mixed dominated
271 aerosol regions. The satellite AOD trends are calculated from the data collocated with
272 AERONET observations.

273 MODIS/ Aqua and MISR AOD at Solar Village have positive trends, while MODIS/ Terra
274 AOD have negative trends along time series (Fig. 4a). MODIS-Aqua AOD differ from those
275 of MODIS-Terra. Discrepancy between Aqua and Terra retrievals could be related to
276 instrument calibration, or the difference in aerosol and cloud conditions from the morning to
277 the afternoon. Both MODIS Aqua and Terra are underestimating AOD at Solar Village.

278 MISR AOD trend shows a better agreement with Solar Village AERONET AOD as
279 compared to MODIS.

280 Both MODIS/Aqua and MODIS/Terra AOD show a stable trend over time at Mezaria site
281 (not shown in the figure) with a correlation coefficient of 0.11 and 0.04 respectively.

282 MODIS/Aqua AOD over Bahrain (not shown in the figure) show, less time trend stability
283 compared to those at Solar Village with a correlation coefficient 0.63. MODIS/Aqua,

284 MODIS/Terra, and MISR AOD depicts a positive trend over Cairo (Fig. 4b). Taman site
285 (Fig. 4c): MODIS/Aqua, MODIS/ Terra, MISR AOD agrees with Taman AERONET on a
286 positive trend indicating data stability over this site.

287 Long-range (2000 – 2015) tendency indicates that contradictory AOD trend of Terra and
288 Aqua is site-dependent and does not necessarily apply everywhere.

289 AOD difference between Terra and Aqua could be used as another indicator of the long-term
290 satellites performance. AOD difference (Terra AOD minus Aqua AOD) varies from -0.01 to

291 0.19, -0.10 to 0.18 over Solar Village, and Taman, respectively (Fig. 5). Over the Solar

Deleted: range

Deleted: , -0.02 to 0.13

Deleted: ,

Deleted: , and Cairo

296 Village, Terra overestimates AOD during 2002-2004 and underestimates the AOD after
297 2005. Taman shows similar trend, however over/underestimation amount is not unique for
298 all sites. This is an indication that Aqua and Terra retrievals disagreement takes place
299 regardless of the region but site sampling has significant effect on the amount of
300 contradiction.

Deleted: Although Cairo and

301 Statistical comparison between MISR and MODIS/Terra AOD at corresponding AERONET
302 stations is performed by calculating G-fraction using $\Delta\tau = \pm 0.05 \pm 0.15\tau_{AERO}$ as a confidence
303 interval. Over the region 1, MISR AOD retrievals are more accurate than MODIS retrievals.
304 MODIS, however, performs better over region 2 sites with high percentage of the data points
305 falling within the confidence range (Tables 2 and 3). High light reflections from the desert
306 landscape surrounding region 1 could have an effect on MODIS retrievals.

Deleted: of

307 Excluding Bahrain and Cairo for low data retrievals the performance of MODIS tends to be
308 similar over all region with ~ 64 percent of AOD retrievals fall within the
309 $\Delta\tau = \pm 0.05 \pm 0.15\tau_{AERO}$ confidence range of the AERONET AOD while MISR retrievals
310 show better performance with ~ 84 percent of the data falling within the same confidence
311 range. This could be attributed to low number of retrievals available for Bahrain and Cairo
312 compared to other sites. Vast sea region surrounding Bahrain and complex landscape in Cairo
313 could also have an impact on retrievals.

314 **4.3 Evaluating the MISR and MODIS climatology over Middle East and North Africa**

315 Comparisons between MISR and MODIS AOD at selected AERONET stations over the
316 2000 – 2015 period are shown in Figures 6- 12.

Deleted: illustrated

317 Figure (6a, b) shows histogram of the MISR, MODIS and AERONET AOD at Solar Village
318 for MISR and MODIS data points collocated with AERONET observations. The mean,
319 standard deviation, and number of measurements are also presented.

323 MISR tends to underestimate the frequency of low AOD compared to AERONET but
324 overestimate the frequency of high AOD. MISR histograms show prominent peaks at 0.50
325 that can be also observed in AERONET and at 0.75 that could not be seen in AERONET.
326 MISR and AERONET AOD climatology agree well with one another. MODIS also tends to
327 underestimate the frequency of low AOD events and overestimate the frequency of high
328 AOD events. High surface reflectance could cause overestimation in MODIS AOD (Ichoku
329 et al., 2005). Both MISR and MODIS provide a good representation of the AOD climatology
330 as compared to AERONET at the Solar Village. Mezaria station, which is located in an arid
331 region in the UAE, has a similar climatology to the Solar Village site with dust dominating
332 aerosol. Figure (7a, b) shows histograms of the MISR, MODIS and AERONET AOD at
333 Mezaria.

334 Similar to the Solar Village, there is a big difference between the number of samples in the
335 matched data set and full AERONET climatology. For MISR there are 213 matched cases
336 and for MODIS there are 498 compared to the 2245 for the entire site. This has an impact on
337 the overall assessment showing significant differences between the matched data and the full
338 climatology for both MISR and MODIS. First, for the MISR case, the matched AERONET
339 data have the highest frequency at AOD of 0.15 and 0.35, but the climatology shows the
340 highest frequency at an AOD of 0.25. AOD in the range of 0.25 to 0.30 are undersampled
341 relative to the climatology, and AOD more than 0.35 matches the climatology with less than
342 2 percent AOD greater than 0.85. MODIS matched AERONET data show prominent peaks
343 at 0.3 and 0.4 compared to the climatology that has a single peak at 0.30.

344 For AOD values between 0.25 and 0.40 MODIS data were found to be under-sampled similar
345 to MISR data between 0.65 to 0.70 and at 0.35.

346 MISR AOD retrievals matched to AERONET capture the variability in the distribution, but
347 as in the case of Solar Village the frequency of low AOD events is underestimated but the

348 frequency of high AOD events matched AERONET data. MISR also captures events with
349 AOD greater than 1. A similar situation is seen in the MODIS comparison, but MODIS
350 appears to do a better job capturing the overall shape of the AERONET AOD histogram for
351 this site.

352 The Bahrain AERONET site is located in Manama fairly close to the Arabian Gulf, a location
353 very different from the previous two sites. The site is also located in an urban area suffers
354 from significant load of anthropogenic aerosols as a consequence of rapid aluminium
355 industrial development (Farahat 2016). Figure (8a, b) shows histogram of the MISR, MODIS
356 and Bahrian AERONET measurements with statistical analysis displayed. The AERONET
357 data matched to MISR show significant peaks at 0.20, 0.30, 0.45, 0.55, 0.7, 0.8, and 0.95 not
358 seen in the all data climatology that has peaks at 0.55 and 0.70. AOD less than 0.15 are not
359 representative in the matched data set at all. MISR is representing the peaks at 0.45 in the
360 matched data set but misses the peaks at 0.20, 0.30, and 0.35. The MISR climatology agrees
361 well with the AERONET all data climatology for all AOD. MODIS on the other hand shows
362 an extremely large frequency of AOD at 0.1 not represented by AERONET coupled with an
363 underestimation of AOD greater than 0.3. This could be attributed to the size of the matching
364 window and MODIS retrievals preferentially coming from the Arabian Gulf.

365 SAADA station is located close to some hiking trails at the Agoundis Valley in the Atlas
366 Mountains about 197 km from the city of Marrakesh.

367 MISR AOD matched to AERONET agree well with MISR full climatology retrievals over
368 SAADA station. Both retrievals slightly underestimate SAADA full climatology and over
369 estimate SAADA matched data retrievals at AOD equal to 0.2 while show good agreement
370 for AOD greater than 0.2. MODIS matched to AERONET retrievals overestimate the
371 frequency of AOD greater than 0.3. While MODIS AOD matched to AERONET captures
372 climatology at AOD between 0.2 to 0.25, AOD frequency retrievals are under-sampled at

373 AOD between 0.1 to 0.15 with about 13 % less events than SAADA all data retrievals at
374 AOD equal to 0.1.

375 Figure (9a, b) indicates right skewed distribution of SAADA AOD towards small AOD
376 values with 10.3 % and 30.1 % of AOD > 0.4 as measured by MISR and MODIS
377 respectively. Taking into consideration MODIS overestimation we conclude that SAADA
378 site is characterized by small AOD values and this could be related to the land topology
379 where the station is located.

380 While MISR is capturing high AOD climatology over SAADA, both MISR and MODIS
381 are underestimating the frequency of lower AOD events. Nevertheless, MISR captures the
382 climatology of AOD less than 0.1 missed by MODIS retrievals.

383 Taman AERONET station is located at the oasis city of Tamanrasset, which lies in Ahaggar
384 National Park in southern Algeria.

385 Figure (10 a, b) depicts that Taman AERONET AOD climatology is similar to those at
386 SAADA and has a high frequency of low AOD events. Both MISR AOD matched to
387 AERONET and MISR all data do not well capture the frequency of AOD less than 0.1 or
388 larger than 1 while well describe the climatology for AOD in the range of 0.1 to 1. MODIS
389 AOD matched data to AERONET correctly describe climatology with slight overestimation
390 of AOD frequencies between 0.05 – 0.15 while not capturing AOD frequencies greater than
391 1. MISR and MODIS show similar prominent peaks at 0.1 and 0.25 not observed in Taman
392 AERONET AOD climatology, with more peaks observed by MISR at 0.5, 0.75, and 0.85.
393 Average AOD in SAADA and Taman is ~ 50 percent less than observed at Solar Village,
394 Mezaria, and Bahrain sites.

395 Except for AOD greater than 1 where ground observations could be more robust, both MISR
396 and MODIS retrievals can provide very good climatology matching over Taman site.

397 Taking into consideration lower number of MISR matching AERONET observations
398 compared to MODIS ~ 21 and 49 percent over SAADA and Taman respectively, MISR is
399 outperforming over these two sites, which can be attributed to its multiangle viewing
400 capabilities over complex terrains including mountainous areas (Atlas Mountains).
401 Cairo is a mega city well known for its high pollution due to traffic and agriculture activities.
402 MISR and MODIS matched data correctly capture AOD climatology over Cairo compared
403 to AERONET as shown in Figure (11a, b). MISR retrievals collocated with AERONET over
404 estimate prominent peaks of AERONET AOD at 0.15 – 0.35 while underestimate
405 AERONET AOD greater than 0.35. MISR ‘all data’ AOD climatology over Cairo station
406 agrees better with AERONET AOD climatology vs. collocated dataset with some
407 oversampling at 0.25. Frequency of high AOD retrievals greater than 0.8 have not been
408 captured by MISR matched or all data retrievals. MODIS matched to AERONET AOD are
409 also able to well represent Cairo climatology data with a high overestimation of AOD
410 frequency between 0.05 - 0.2 and an underestimation of AOD larger than 0.4.
411 The complex landscape and local emissions in Cairo could impose major challenges in
412 MODIS AOD retrievals. Moreover, Cairo is one of the most densely populated cities in the
413 world that hosts major commercial and industrial centers in North Africa. Cairo also has
414 complicated aerosols structure developed by long range transported dust in the spring,
415 biomass burning in the fall, strong traffic and industrial emissions (Marey et al., 2010).
416 Over Cairo station, MODIS correctly represents ground observations for AOD between 0.2
417 - 0.4 while MISR all data better represents AOD climatology for AOD greater than 0.4.
418
419 MISR, MODIS climatology at SEDEE Boker are illustrated in Figures (12a, b).
420 MISR ‘matched’ AOD frequency show significant underestimation for AOD less than 0.2
421 and an overestimation between 0.2 – 0.4 compared with AERONET retrievals. MISR

422 correctly captures the climatology for AOD events greater than 0.4. MISR ‘matched’ and ‘all
423 data’ retrievals peaks at 0.2 producing high frequency of AOD oversampling compared to
424 AERONET. MISR data retrievals do not capture the climatology for AOD less than 0.1 over
425 this site coincident with what was previously observed over other sites. MODIS matched
426 AERONET data underestimates frequency of AOD less than 0.2 while overestimates the
427 frequencies between 0.2 - 0.6, and well match frequencies of higher AOD events larger than
428 0.6. MODIS retrievals are characterized by two prominent peaks at 0.1 and 0.25 that are not
429 found in the AERONET matched data.

430 At Sedee, MISR and MODIS retrievals are better in matching frequency of high AOD
431 retrievals (greater than 0.4) than the frequency of low AOD. This could be an effect of
432 possible long-range transport to Sedee Boker site (Farahat et al. 2016) along with complex
433 mixtures of dust, pollution, smoke, and sea salt that could result in uncertainties in MISR and
434 MODIS aerosol model selection.

435 In the summary, MISR tends to overestimate AOD > 0.4 over Solar Village, Bahrain and
436 underestimate AOD > 0.4 over Cairo. MISR retrievals also match AOD > 0.4 for Mezaria
437 and Sedee Boker, while agree with AERONET over SAADA and Taman at all ranges of
438 AOD. This could be expounded by insufficient particle absorption in MISR algorithm (Kahn
439 et al., 2005). Spherical particle absorption is produced by externally mixing small black
440 carbon particles.

441 Percentage of MISR, MODIS, and AERONET AOD greater than 0.4 recorded is shown in
442 Table 4. Over Solar Village, both MISR and MODIS well capture high AOD greater than
443 0.4 with very good agreement with the ground observations. Over Mezaria, both MISR and
444 MODIS are over estimating the percentage of AOD greater than 0.4 by about 17.7 and 12.7
445 percent respectively. MISR all data agrees well with AERONET all data in representing high
446 AOD over Bahrain while MODIS shows significant under-representation of those events by

447 about 13 percent, less than reported by Bahrain AERONET station. At SAADA, MISR AOD
448 agrees with AERONET in showing low percentage of AOD greater than 0.4, while MODIS
449 retrievals overestimate percentage by about 24 percent. MISR AOD over Taman AERONET
450 station shows very good agreement, while MODIS is slightly underestimating AOD. Among
451 all seven sites considered in this study, Sedee Boker shows lowest occurrence of AOD greater
452 than 0.4, which is confirmed by both MISR and MODIS retrievals. Cairo AERONET records
453 the highest frequency of AOD > 0.4, however this is largely underestimated by both MISR
454 and MODIS retrievals.

455 It can be concluded from the previous discussion that the atmosphere around SAADA,
456 Taman, and Sedee Boker sites is relatively clean and aerosol loads are small compared to
457 Solar Village, Mezaria, Bahrain, and Cairo, however this could be affected by the location
458 where AERONET station is installed for example SAADA and Taman stations are installed
459 in a remote mountainous region away from urbanization while Cairo station is installed in
460 the middle of large residential region with significant local emissions.

461

462 **Conclusion**

463 The performance of MODIS, MISR retrievals with corresponding AERONET
464 measurements over different geographic locations in the Middle East and North Africa was
465 investigated during 2000 – 2015.

466 Long-~~term~~ observations show dissimilar AOD trends between MODIS/Aqua,
467 MODIS/Terra, MISR and AERONET measurements. MODIS/Aqua matched AERONET
468 retrievals show stable trend over all sites while, MODIS/Terra matched AERONET retrievals
469 show significant downward trend indicating possible changes in the sensor performance.

Deleted: range

471 MISR matched AERONET AOD data depict high correlation compared to
472 AERONET indicating good agreement with ground observations with about 84 percent of
473 AOD retrievals fall within the expected confidence range.

474 Consistency of MODIS and AERONET AOD vary based on the season, study area,
475 and dominant aerosols type with about 64 percent of the retrieved AOD values fall within
476 expected confidence range with the lowest performance over mixed particles regions.

477 Comparing satellites' AOD retrievals with corresponding AERONET measurements
478 show that space-borne data retrievals accuracy can be affected by landscape, topology, and
479 AOD range at which data is retrieved.

480 Few AERONET sites are verified where MISR and MODIS retrievals agree well with
481 ground observations, while other sites only MISR or MODIS could correctly describe the
482 climatology.

483 The AOD range at which MISR or MODIS could correctly describe ground
484 observation is also investigated over different AERONET sites. Over Solar Village both
485 MISR and MODIS tend to underestimate the frequency of low AOD and overestimate the
486 frequency of high AOD compared to AERONET with MISR histograms show prominent
487 peaks at 0.50 that matched AERONET data and 0.75 that could not be recorded in
488 AERONET. MISR can capture the frequency of AOD greater than 1 mostly missed by
489 MODIS. Both MISR and MODIS are found to provide good representation of the AOD
490 climatology over the Solar Village site.

491 Similar to Solar Village, MISR underestimates frequency of lower AOD and
492 overestimate frequencies of high AOD over Mezaria. MISR is able to correctly capture the
493 frequency of AOD greater than 1, while MODIS retrievals are found to better represent the
494 overall climatology. This is due to low number of MISR – matched AERONET retrievals

495 compared to MODIS over this site. Prominent peaks at 0.3 and 0.4 were observed in MODIS
496 matched Mezaria retrievals compared to the climatology, which has a single peak at 0.30.

497 Large water body surrounding Bahrain makes MODIS data preferentially originate
498 from the Arabian Gulf which produces an extremely large frequency of AOD at 0.1 not
499 observed in AERONET measurements paired with an underestimation of AOD greater than
500 0.3. Meanwhile, MISR retrievals agree well with AOD climatology over Bahrain.

501 MISR AOD retrievals slightly underestimate SAADA climatology while they show good
502 agreement for AOD greater than 0.1. MODIS retrievals underestimate the frequency of AOD
503 retrievals between 0.1 to 0.15, match climatology at AOD between 0.2 to 0.25, and
504 overestimate the frequency of AOD greater than 0.3. SAADA site is characterized by small
505 frequency of low AOD values and this could be related to the landscape nature surrounding
506 Saada station. MISR is found to be outperforming over Saada and Taman stations which can
507 be attributed to its viewing multispectral and multiangular capabilities over mountainous
508 regions.

509 MISR retrievals well capture prominent peaks of AERONET data at 0.15 to 0.35
510 with small underestimation observed at AOD greater than 0.3 over Cairo. Using either MISR
511 matched data or MISR all data over Cairo was found to perform well in describing the
512 climatology over this station. MODIS data retrievals are also able to well represent Cairo
513 climatology with a high overestimation of AOD frequency between 0.05 to 0.2 and an
514 underestimation of AOD larger than 0.4. While both MISR and MODIS well describe
515 climatology over Cairo station, MODIS can correctly represent ground observations between
516 0.2 to 0.4.

517 Over Sedee Boker both MISR and MODIS retrievals well describe the climatology however
518 they are more successful in matching frequency of high AOD greater than 0.4.

Deleted: do a good job

520 Based on analysing frequency of AOD greater than 0.4, it was found that Saada, Taman, and
521 Sedee Boker are having better air quality compared to other sites while Cairo was found to
522 be the most polluted site.

523 Results presented in this study are important in providing a guideline for satellites retrievals
524 end users on which sensor could provide reliable data over certain geographic location and
525 AOD range.

526 Adjacent geographic location and local climate among sites does not always
527 guarantee that same sensor will provide consistent retrievals over all sites. For example, Solar
528 Village, and Bahrain AERONET are surrounded by large desert regions and sharing almost
529 similar climatic conditions, but MODIS is found to be more successful in describing
530 climatology over Solar Village than over Bahrain and this could be attributed to different
531 factors related to surface reflection, cloud coverage, and the large water body surrounding
532 Bahrain. Thus in order to decrease data uncertainty, it is important to determine which sensor
533 provides best retrieval over certain geographic location and AOD range.

534

535 **Acknowledgements**

536 The author would like to acknowledge the support provided by the Deanship of Scientific
537 Research (DSR) at the King Fahd University of Petroleum and Minerals (KFUPM) for
538 funding this work through project # IN161053. Portions of this work were performed at the
539 Jet Propulsion Laboratory (JPL), California Institute of Technology, under a contract with
540 the National Aeronautics and Space Administration. The author would like to thank Michael
541 Garay (MJG) and Olga Kalashnikova (OVK) (JPL) for their suggestion of investigating
542 satellites – AERONET matched data climatology, and discussion during the data analysis.
543 The author would also like to thank Hesham El-Askary (Chapman University) for providing
544 recommendation about AERONET data over North Africa and the Middle East as well as
545 reviewing the English in the manuscript. We thank the MISR project for providing facilities,
546 and supporting contributions of MJG and OVK. Finally, we thank the reviewers for
547 suggestions, which improved the manuscript.

548

549
550
551
552
553
554
555
556
557
558
559
560
561
562
563
564
565
566
567
568
569
570
571
572
573
574
575
576
577
578
579
580
581
582
583
584
585
586
587
588
589
590
591
592
593

Author Contributions: Ashraf Farahat analysed the data, performed the statistical analysis and wrote the manuscript.

Conflicts of Interest: The authors declare no conflict of interest.

References

1. Abdi, V., Flamant, C., Cuesta, J., Oolman, L., Flamant, P., and Khalesifard, H. R. Dust transport over Iraq and northwest Iran associated with winter Shamal: A case study. *J. Geophys. Res.*, 117, D03201, 2013.
2. Ackerman, S., Strabala, K. I., Menzel, W. P., Frey, R. A., Moeller, C. C. and Gumley, L. E. (1998): Discriminating clear sky from clouds with MODIS. *J. Geophys. Res.*, 103, 32 141–157, 1998.
3. Afnan, F. Heavy metal, trace element and petroleum hydrocarbon pollution in the Arabian Gulf: Review, *Journal of the Association of Arab Universities for Basic and Applied Sciences*, 17, 90-100, 2015.
4. Ansmann, A., Petzold, A., Kandler, K., Tegen, I., Wendisch, M., Müller, D., Weinzierl, B., Müller, T., and Heintzenberg, J. Saharan Mineral Dust Experiments SAMUM-1 and SAMUM-2: what have we learned? *Tellus B*, 63, 403–429, 2011.
5. Basart, S., Pérez, C., Cuevas, E., Baldasano, J. M., and Gobbi., G. P. Aerosol characterization in Northern Africa, Northeastern Atlantic, Mediterranean Basin and Middle East from direct-sun AERONET observations. *Atmos. Chem. Phys.*, 9, 8265-8282, 2009.
6. Böer B., An introduction to the climate of the United Arab Emirates (review). *J Arid Environ*, 35:3–16, 1997.
7. Bou Karam, D., Flamant, C., Cuesta, J., Pelon, J., and Williams, E. Dust emission and transport associated with a Saharan depression: February 2007 case, *J. Geophys. Res.*, 115, D00H27, 2010.
8. Breón, F-M., Vermeulen, A., Descloitres, J. An evaluation of satellite aerosol products against sunphotometer measurements. *Remote Sensing Environ.*, 115, 3102–11, 2011.

- 594 9. Bruegge, C., Chrien, N., Kahn, R., Martonchik, J., and Diner, D. MISR radiometric
595 uncertainty analyses and their utilization within geophysical retrievals. *IEEE Trans.*
596 *Geosci. Remote Sens.*, 36, 1186- 1198, 1998.
- 597
598
- 599 10. Chin, M., Diehl, T., Tan, Q., Prospero, J. M., Kahn, R. A., Remer, L. A., Yu, H.,
600 Sayer, A. M., Bian, H., Geogdzhayev, I. V., Holben, B. N., Howell, S. G.,
601 Huebert, B. J., Hsu, N. C., Kim, D., Kucsera, T. L., Levy, R. C.,
602 Mishchenko, M. I., Pan, X., Quinn, P. K., Schuster, G. L., Streets, D. G.,
603 Strode, S. A., Torres, O., and Zhao, X.-P. Multi-decadal aerosol variations from
604 1980 to 2009: a perspective from observations and a global model, *Atmos. Chem.*
605 *Phys.*, 14, 3657-3690, 2014.
- 606
- 607 11. Chu, D. A., Kaufman, Y. J., Remer, L. A., and Holben, B. N. Remote sensing of
608 smoke from MODIS airborne simulator during the SCAR-B experiment. *J. Geophys.*
609 *Res.*, 103, 31, 979– 987, 1998.
- 610
- 611 12. Derimian, Y., Karnieli, A., Kaufman, Y. J., Andreae, M. O., Andreae, T. W.,
612 Dubovik, O., Maenhaut, W., Koren, I., and Holben, B. N. Dust and pollution
613 aerosols over the Negev desert, Israel: Properties, transport, and radiative effect. *J.*
614 *Geophys. Res.*, 111, D05205, 2006.
- 615
- 616 13. Dubovik, O. and King, M. D. A flexible inversion algorithm for retrieval of aerosol
617 optical properties from Sun and sky radiance measurements. *J. Geophys. Res.*, 105
618 206730–20696, 2000.
- 619
- 620 14. Dubovik, O., Holben, B. N., Eck, T. F., Smirnov, A., Kaufman, Y. J., King, M. D.
621 Tanre, D., and Slutsker, I. Variability of absorption and optical properties of key
622 aerosol types observed in worldwide locations. *J. Atmos. Sci.*, 59, 590–608, 2002.
- 623
- 624 15. Dubovik, O., Sinyuk, A., Lapyonok, T., Holben, B., Mischenko, M., Yang, P., Eck,
625 T., Volten, H., Muñoz, O., Veihelmann, B., van der Zande, W. J., Leon, J.-F.,
626 Sorokin, M., and Slutsker, I. The application of spheroid models to account for
627 aerosol particle non-sphericity in remote sensing of desert dust. *J. Geophys. Res.*,
628 111, D11208, 2006.
- 629
- 630 16. Eck, T., Holben, B. N., Reid, J. S., O’Neill, N. T., Schafer, J. S., Dubovik, O.,
631 Smirnov, A., Yamasoe, M. A., and Artaxo, P. High aerosol optical depth biomass
632 burning events: A comparison of optical properties for different source regions,
633 *Geophys. Res. Lett.*, 200b, 30, 20, 2035, 2003b.
- 634
- 635 17. Eck, T., et al. Climatological aspects of the optical properties of fine/coarse mode
636 aerosol mixtures. *J. Geophys. Res.*, 115, D19205, 2010.
- 637
- 638 18. Elagib, N., Addin Abdu A. Climate variability and aridity in Bahrain. *J. Arid*
639 *Environ.*, 36:405–419, 1997.
- 640

- 641 19. El-Askary H., Farouk R., Ichoku C., and Kafatos M. Inter-continental transport of
642 dust and pollution aerosols across Alexandria, Egypt, *Annales Geophysicae*, 27,
643 2869–2879, 2009.
- 645 20. Farahat, A., El-Askary, H., and Al-Shaibani, A. Study of Aerosols' Characteristics
646 and Dynamics over the Kingdom of Saudi Arabia using a Multi Sensor Approach
647 Combined with Ground Observations. *Advances in Meteorology*, Article ID
648 247531, 2015.
- 650 21. Farahat, A. Air Pollution in Arabian Peninsula (Saudi Arabia, United Arab
651 Emirates, Kuwait, Qatar, Bahrain, and Oman): Causes, Effects and Aerosol
652 Categorization. *Arab J of Geosci.*, 9, 196, 2016.
- 654 22. Farahat, A., El-Askary, H., and Dogan, A. U., 2016: Aerosols size distribution
655 characteristics and role of precipitation during dust storm formation over Saudi
656 Arabia. *Aerosol Air Qual. Res.*, 16, 2523-2534, 2016.
- 658 23. Farahat, A., El-Askary, H., Adetokunbo, P., Abu-Tharr, F. Analysis of aerosol
659 absorption properties and transport over North Africa and the Middle East using
660 AERONET data. *Annales Geophysicae.*, 34:11, 1031-1044, 2016.
- 662 24. He, Q., Li, C., Tang, X., Li, H., Geng, F., Wu, Y. Validation of MODIS derived
663 aerosol optical depth over the Yangtze River Delta in China. *Remote Sensing
664 Environ.*, 114, w21649–61, 2010.
- 665 25. Higurashi, A., and Nakjima, T. Development of a two-channel aerosol retrieval
666 algorithm on a global scale using NOAA AVHRR. *J. Atmos. Sci.*, 56, 924–941,
667 1999.
- 669 26. Holben, B., Eck, T., Slutsker, I., Tanre, D., Buis, J., Setzer, A. et al. AERONET—
670 A federated instrument network and data archive for aerosol characterization.
671 *Remote Sensing Environ.*, 66, 1–16, 1998.
- 674 27. Holben, B., Smirnov, A., Eck, T., Slutsker, I., Abuhassan, N., Newcomb, W., et al.
675 An emerging ground-based aerosol climatology—Aerosol optical depth from
676 AERONET, *J. Geophys Res.*, 106, 12067–97, 2001.
- 678 28. Hoell, A., Funk, C., and Barlow, M. The regional forcing of Northern Hemisphere
679 drought during recent warm tropical west Pacific Ocean La Niña events. *Clim.
680 Dyn.*, 42, 3289–3311, 2013.
- 682 29. Hsu, N., Gautam, R., Sayer, A., Bettenhausen, C., Li, C., Jeong, M., Tsay, S., and
683 Holben, B. Global and regional trends of aerosol optical depth over land and ocean
684 using SeaWiFS measurements from 1997 to 2012. *Atmos. Chem. Phys.*, 12, 8037–
685 8053, 2012.
- 687

- 688 30. Ichoku, C., Chu, D. A., Mattoo, S., Kaufman, Y. J., Remer, L. A., Tanre, D.,
689 Slutsker, I., and Holben, B. N. A spatio-temporal approach for global validation
690 and analysis of MODIS aerosol product, *Geophys. Res. Lett.*, 29, 12, 8006, 2002.
691
- 692 31. Ginoux, P., Chin, M., Tegen, I., Prospero, J., Holben, B., Dubovik, O., and Lin, S.-
693 J. Sources and global distributions of dust aerosols simulated with the GOCART
694 model, *J. Geophys. Res.*, 106, 20255 – 20273, 2001.
695
- 696 32. Kahn, R. A., Gaitley, B. J., Martonchik, J. V., Diner, D. J., Crean, K. A. and Holben,
697 B. Multiangle ImagingSpectroradiometer (MISR) global aerosol optical depth
698 validation based on 2 years of coincident Aerosol Robotic Network (AERONET)
699 observations, *J. Geophys. Res.*, 110, 2005.
700
- 701 33. Kahn, R., Garay, M., Nelson, D., Yau, K., Bull, M., Gaitley, B. et al. Satellite-
702 derived aerosol optical depth over dark water from MISR and MODIS:
703 Comparisons with AERONET and implications for climatological studies. *J.*
704 *Geophys. Res.*, 112, D18205, 2007.
705
- 706 34. Kahn, R., Nelson, D., Garay, M., Levy, R., Bull, M., Diner, D., et al. MISR aerosol
707 product attributes, and statistical comparisons with MODIS. *IEEE Trans Geosci*
708 *Remote Sensing*, 47, 4095–114, 2009.
709
- 710 35. Kim, D., Chin, M., Bian, H., Tan, Q., Brown, M. E., Zheng, T., You, R., Diehl, T.,
711 Ginoux, P., and Kucsera, T. The effect of the dynamic surface bareness on dust
712 source function, emission, and distribution, *J. Geophys. Res.*, 118, 1–16, 2013.
713
- 714 36. Kaufman, Y., Tanre, D., Remer, L., Vermote, E., Chu, A., and Holben, B.
715 Operational remote sensing of tropospheric aerosol over land from EOS moderate
716 resolution imaging spectroradiometer. *J. Geophys. Res.-Atmos.*, 102, D14, 17051–
717 17067, 1997.
718
- 719 37. Kokhanovsky, A., Breon, F., Cacciari, A., Carboni, E., Diner, D., Di Nicolantonio,
720 W. et al. Aerosol remote sensing over land: a comparison of satellite retrievals using
721 different algorithms and instruments. *Atmos Res.*, 85, 372–94, 2007.
722
- 723 38. Liu, L., Mishchenko, M. Toward unified satellite climatology of aerosol properties:
724 direct comparisons of advanced level 2 aerosol products. *JQSRT.*, 109, 2376–85,
725 2008.
726
- 727 39. Marey, H., Gille, J., El-Askary, H., Shalaby, E. , and El- Raey, M. Study of the
728 formation of the “black cloud and its dynamics over Cairo, Egypt, using MODIS
729 and MISR sensors. *J. Geophys. Res.*, 115, D21206, 2010.
730
- 731 40. Martonchik, J., Diner, D., Crean, K., and Bull, M. Regional aerosol retrieval results
732 from MISR. *IEEE Trans. Geosci. Remote Sens.*, 40, 1,520–1,531, 2002.
733
- 734 41. Mishchenko, M., I. Geogdzhayev, L. Liu, A. Lacis, B. Cairns, L. Travis. Toward
735 unified satellite climatology of aerosol properties: what do fully compatible
736 MODIS and MISR aerosol pixels tell us? *J Quant Spectrosc Radiat Transfer.* 110,
737 402–8, 2009.

- 738
739 42. Mishchenko, M., Liu, L., Geogdzhayev, I., Travis, L., Cairns, B., Lacic, A. Toward
740 unified satellite climatology of aerosol properties: 3. MODIS versus MISR versus
741 AERONET. *J Quant Spectrosc Radiat Transfer.*, 111, 540–52, 2010.
742
- 743 43. Remer, L., Kaufman, Y., Tanre´, D., Mattoo, S., Chu, D., Martins, J., et al. The MODIS
744 aerosol algorithm, products, and validation. *J Atmos Sci.*, 62, 947–73, 2005.
745
- 746 44. Sadiq, M. and McCain, J. *The Gulf War Aftermath: An Environmental Tragedy.*,
747 1st ed., Springer, 1993.
748
- 749 45. Sayer, A., Hsu, N., Eck, T., Smirnov, A., and Holben, B. AERONET-based models
750 of smoke-dominated aerosol near source regions and transported over oceans, and
751 implications for satellite retrievals of aerosol optical depth. *Atmos. Chem. Phys.*,
752 14, 11493-11523, 2014.
753
- 754 46. Schepanski, K., Mallet, M., Heinold, B., and Ulrich, M.: North African dust
755 transport toward the western Mediterranean basin: atmospheric controls on dust
756 source activation and transport pathways during June–July 2013, *Atmos. Chem.*
757 *Phys.*, 16, 14147-14168, 2016.
758
- 759 47. Sioris, C. E., McLinden, C. A., Shephard, M. W., Fioletov, V. E., and Abboud, I.:
760 Assessment of the aerosol optical depths measured by satellite-based passive
761 remote sensors in the Alberta oil sands region, *Atmos. Chem. Phys.*, 1931-1943,
762 2017.
763
- 764 48. Smirnov, A., Holben, B., Eck, T., Dubovik, O., and Slutsker, I. Cloud-screening
765 and quality control algorithms for the AERONET data-base, *Remote Sens.*
766 *Environ.*, 73, 337 – 349, 2000.
767
- 768 49. Solomos, S., Ansmann, A., Mamouri, R.-E., Biniotoglou, I., Patlakas, P., Marinou,
769 E., and Amiridis, V. Remote sensing and modelling analysis of the extreme dust
770 storm hitting the Middle East and eastern Mediterranean in September 2015,
771 *Atmos. Chem. Phys.*, 17, 4063-4079, 2017.
772
- 773 50. Todd M., R. Washington, Vanderlei, M., Dubovik, O., Lizcano, G., M’Bainayel,
774 S., Engelstaedter, S. Mineral dust emission from the Bodélé Depression, northern
775 Chad, during BoDEx 2005. *J. Geophys. Res.*, 112. D06207, 2007.
776
- 777 51. Von Hoyningen-Huene, W., Posse, P. Nonsphericity of aerosol particles and their
778 contribution to radiative forcing. *JQSRT*, 57, 651–68, 1997.
779
780
- 781 52. Yu, Y., Notaro, M., Liu, Z., Kalashnikova, O., Alkolibi, F., Fadda, E., and Bakhrjy,
782 F. Assessing temporal and spatial variations in atmospheric dust over Saudi Arabia
783 through satellite, radiometric, and station data, *J. Geophys. Res. Atmos.*, 118, 13,
784 253–13, 264, 2013.
785

786 53. Yu, Y., Notaro, M., Liu, Z., Wang, F., Alkolibi, F., Fadda, E. and Bakhry,
787 F. Climatic controls on the interannual to decadal variability in Saudi Arabian dust
788 activity: Toward the development of a seasonal dust prediction model. *J. Geophys.*
789 *Res. Atmos.*, 120, 1739–1758, 2015.

791 54. Zhao, G. and Girolamo, L. A cloud fraction versus view angle technique for
792 automatic in-scene evaluation of the MISR cloud mask. *J. Appl. Meteorol.*, 43, 6,
793 860–869, 2004.

794

795

796

797

798

799

800

801

802

803

804

805

806

807

808

809

810

811

812

813

814

815 **Tables' caption**

816 Table 1. Geographic location of the AERONET sites used in this study

817 Table 2. Statistics for dust sites, R: correlation coefficient, RMSE: Root Mean Square

818 deviation; G-fraction: good fraction; N: number of observations

819 Table 3. Statistics for biomass and mixed sites, parameters as in Table 3. Caption.

820 Table 4. MISR coverage for six days of major dust activity over the Arabian Peninsula

821 during March 2009.

822

823

824

825

826

827

828

829

830

831

832

833

834

835

836

837

838

839

840 **Figures caption**

841 Figure 1. Location of the AERONET stations over North Africa and the Middle East. The
842 numbers on the map indicates the site location as 1: Saada, 2: Tamanrasset_INM, 3: Cairo,
843 4: Sede Boker, 5: Solar Village, 6: Mezaira, 7: Bahrain.

844 Figure 2. Scatter plot of MISR AOD versus AERONET AOD based on seasons and
845 aerosols categorization.

846 Figure 3. Scatter plot of MODIS AOD versus AERONET AOD based on seasons and
847 aerosols categorization.

848 Figure 4. Time series of monthly mean AOD derived from MODIS/Aqua, MODIS/Terra,
849 MISR and AERONET over a) dust b) biomass and c) mixed dominated aerosol regions.

850 Figure 5. Long-term AOD difference for MODIS/Terra and MODIS/Aqua over the Solar
851 Village and Taman sites.

852 Figure 6. Histogram of the MISR, MODIS and Solar Village AERONET measurements a)
853 MISR b) MODIS data retrievals.

854 Figure 7. Histogram of the MISR, MODIS and Mezaria AERONET measurements a)
855 MISR b) MODIS data retrievals.

856 Figure 8. Histogram of the MISR, MODIS and Bahrain AERONET measurements a) MISR
857 b) MODIS data retrievals.

858 Figure 9. Histogram of the MISR, MODIS and SAADA AERONET measurements a)
859 MISR b) MODIS data retrievals.

860 Figure 10. Histogram of the MISR, MODIS and Taman AERONET measurements a)
861 MISR b) MODIS data retrievals.

862 Figure 11. Histogram of the MISR, MODIS and SEDEE Boker AERONET measurements
863 a) MISR b) MODIS data retrievals.

Deleted: range

Deleted: dust

Deleted: , biomass

Deleted: mixed

868 Figure 12. Histogram of the MISR, MODIS and Cairo AERONET measurements a) MISR

869 b) MODIS data retrievals.

870

871

872

873

874

875

876

877

878

879

880

881

882

883

884

885

886

887

888

889

890

891

892

893

Table 1.

Location name	Lon./Lat.	Measurement period
Solar Village	24.907° N/46.397° E	2000-2015
Mezaria	23.105° N/53.755° E	2004-2015
Bahrain	26.208° N/50.609° E	2000-2006
Saada	31.626° N/8.156° W	2003-2015
Taman	22.790° N/5.530° E	2000-2015
Cairo (EMA 2)	30.081° N/31.290° E	2010-2017
Sede Boker	30.855° N/34.782 ° E	2000-2015

Formatted: Font: 10 pt, Complex Script Font: 10 pt

Deleted: 2005

Deleted: 0

894

895

896

897

898

899

900

901

902

903

904

905

906

907

908

909

910

Table 2.

AERONET	Sensor	Season	Mean Value	N	R	Gfraction (%)	
Site			AERONET	Satellite			
Solar Village	MISR	DJF	0.18±0.15	0.23±0.13	24	0.94	79.1
		MAM	0.45±0.21	0.47±0.20	43	0.94	86.0
		JJA	0.39±0.16	0.42±0.16	57	0.90	82.4
		SON	0.25±0.14	0.29±0.12	50	0.99	82.0
	MODIS Terra	DJF	0.27±0.19	0.33±0.17	1500	0.48	51.80
		MAM	0.36±0.24	0.26±0.17	389	0.68	90.23
		JJA	0.34±0.17	0.42±0.19	429	0.41	54.31
		SON	0.22±0.10	0.36±0.12	471	0.51	28.87
Mezaria	MISR	DJF	0.17±0.09	0.23±0.07	53	0.89	50.9
		MAM	0.34±0.18	0.37±0.18	41	0.90	78.0
		JJA	0.49±0.20	0.47±0.21	51	0.85	92.1
		SON	0.26±0.09	0.30±0.12	53	0.87	88.2
	MODIS Terra	DJF	0.32±0.15	0.35±0.19	198	0.86	74.74
		MAM	0.44±0.33	0.45±0.27	115	0.92	78.07
		JJA	0.39±0.14	0.43±0.20	89	0.81	71.91
		SON	0.28±0.13	0.30±0.16	97	0.87	77.31
Bahrain	MISR	DJF	0.19±0.10	0.30±0.10	9	0.73	33.3
		MAM	0.47±0.20	0.67±0.05	7	0.89	28.5
		JJA	0.45±0.21	0.74±0.21	21	0.69	23.8
		SON	0.32±0.13	0.45±0.16	22	0.98	45.4
	MODIS Terra	DJF	0.42±0.29	0.20±0.19	121	0.41	93.38
		MAM	0.50±0.28	0.13±0.15	25	0.26	96.00
		JJA	0.55±0.26	0.31±0.27	42	0.50	88.09
		SON	0.35±0.14	0.21±0.12	29	0.32	93.10

Table 3.

AERONET Site	Method	Season	Mean Value	N	R	Gfraction (%)		
			AERONET	Satellite				
SAADA	MISR	DJF	0.07±0.02	0.07±0.02	43	0.93	100.0	
		MAM	0.17±0.10	0.17±0.09	47	0.89	93.6	
		JJA	0.30±0.14	0.31±0.14	53	0.93	93.1	
		SON	0.14±0.07	0.13±0.06	51	0.94	96.0	
	MODIS	DJF	0.23±0.16	0.32±0.21	550	0.57	57.8	
		MAM	0.24±0.18	0.39±0.23	90	0.43	44.4	
		JJA	0.30±0.17	0.45±0.18	201	0.40	45.2	
		SON	0.19±0.13	0.22±0.14	162	0.71	72.3	
	Taman	MISR	DJF	0.07±0.10	0.09±0.06	69	0.92	85.5
			MAM	0.22±0.18	0.25±0.22	86	0.97	81.3
			JJA	0.42±0.31	0.45±0.28	57	0.85	78.9
			SON	0.14±0.11	0.15±0.10	72	0.94	95.8
MODIS		DJF	0.19±0.22	0.18±0.16	319	0.67	81.8	
		MAM	0.24±0.19	0.22±0.17	67	0.55	83.5	
		JJA	0.37±0.32	0.29±0.20	69	0.69	84.0	
		SON	0.14±0.14	0.13±0.10	117	0.54	84.6	
Cairo	MISR	DJF	0.33±0.17	0.17±0.09	15	0.94	100.0	
		MAM	0.35±0.13	0.33±0.15	39	0.99	82.0	
		JJA	0.35±0.09	0.27±0.08	61	0.99	96.7	
		SON	0.37±0.14	0.28±0.13	23	0.97	78.2	
	MODIS	DJF	0.33±0.16	0.20±0.11	158	0.30	95.5	
		MAM	0.32±0.16	0.12±0.08	39	0.25	100.0	
		JJA	0.35±0.14	0.28±0.07	58	0.17	94.8	
		SON	0.38±0.19	0.20±0.09	29	0.07	93.8	

	DJF	0.11±0.06	0.13±0.05	10	0.87	90.0
	MAM	0.21±0.13	0.24±0.13	76	0.68	75.0
MISR	JJA	0.16±0.08	0.21±0.08	142	0.85	66.9
	SON	0.162±0.07	0.20±0.06	54	0.89	79.6
SEDEE_BOKER	DJF	0.16±0.12	0.23±0.14	1312	0.36	53.5
	MAM	0.21±0.18	0.24±0.19	338	0.34	65.6
MODIS	JJA	0.16±0.09	0.33±0.13	392	0.27	17.3
Terra	SON	0.16±0.09	0.23±0.12	477	0.46	58.4

918

919

920

921

922

923

924

925

926

927

928

929

930

931

932

933

934

935

936

937

Table 4.

	AERONET		MISR		MODIS	
	AOD		AOD		AOD	
	N	% > 0.4	N	% > 0.4	N	% > 0.4
Solar	3893	27.17	684	32.8	2789	30.1
Village						
Mezaria	2245	28.01	547	45.7	498	40.7
Bahrain	1116	31.36	676	35.8	217	18.4
SAADA	2974	10.32	667	11.5	1004	34.6
Taman	798	15.78	845	22.6	572	9.4
Cairo	2222	38.79	620	17.7	284	4.2
SEDEE	5722	4.28	675	9.0	2519	12.8

938

939

940

941

942

943

944

945

946

947

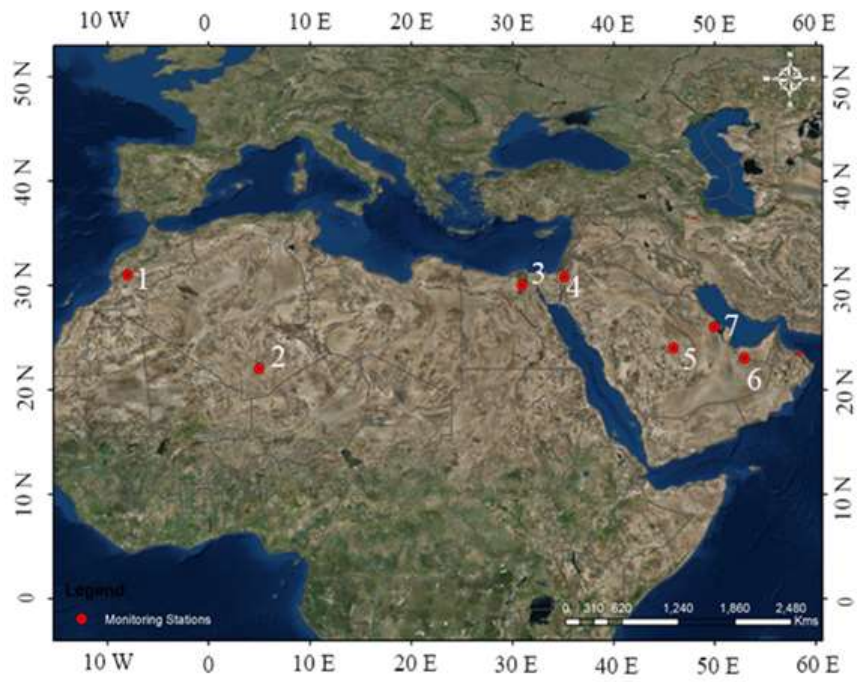
948

949

950

951

952



953

954

955 Figure 1.

956

957

958

959

960

961

962

963

Region 1

Region 2

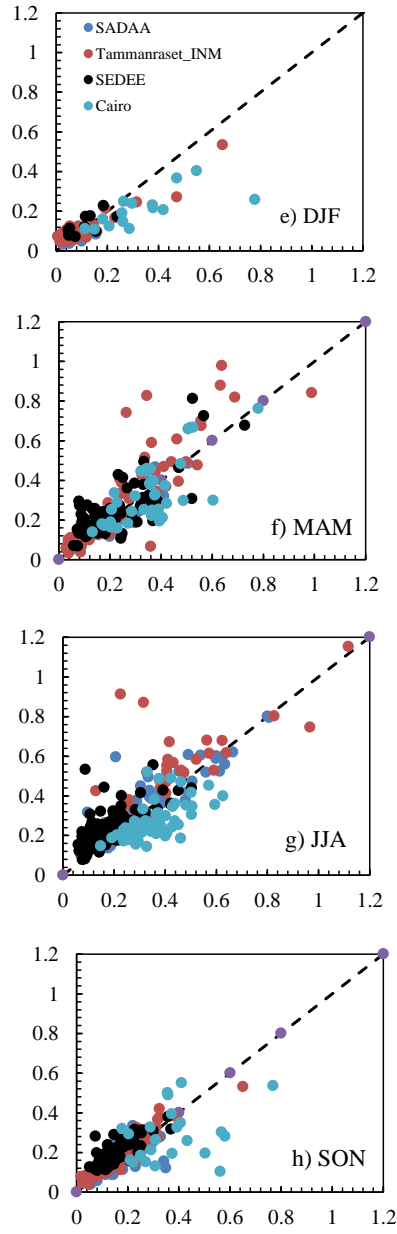
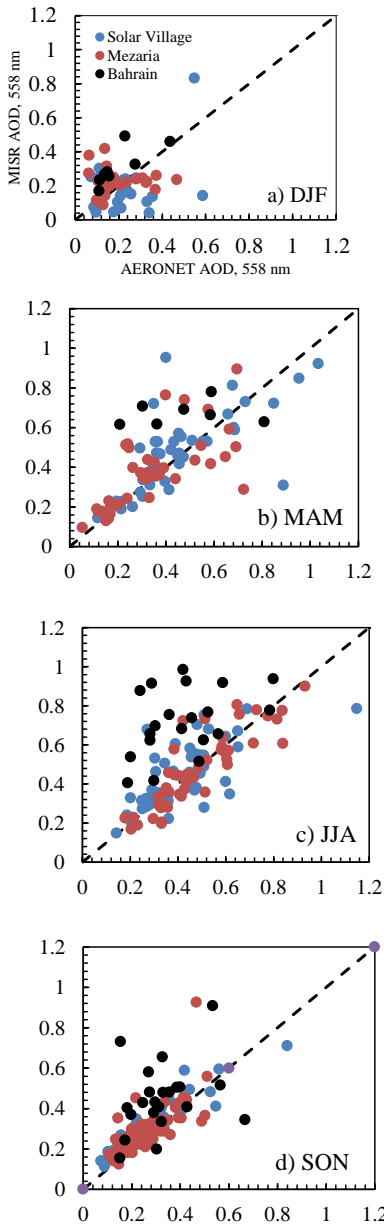
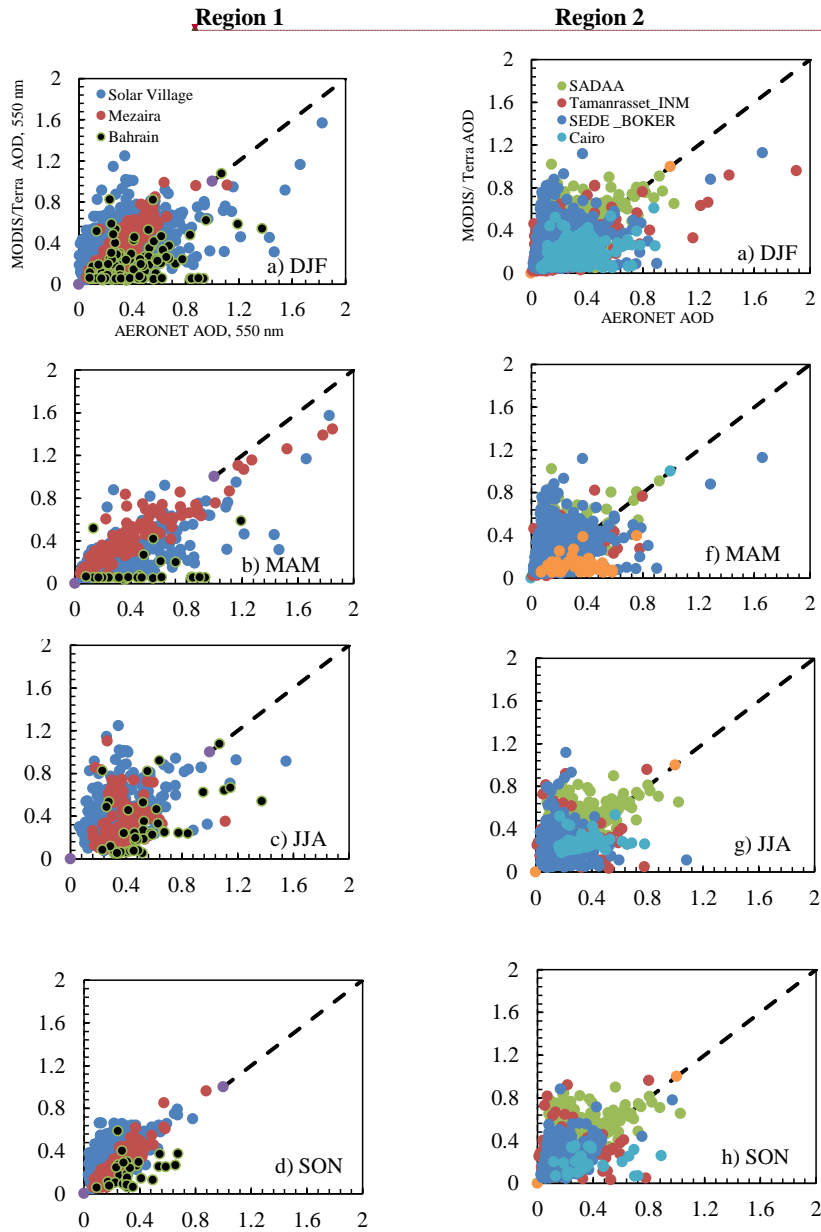


Figure 2

Moved (insertion) [1]



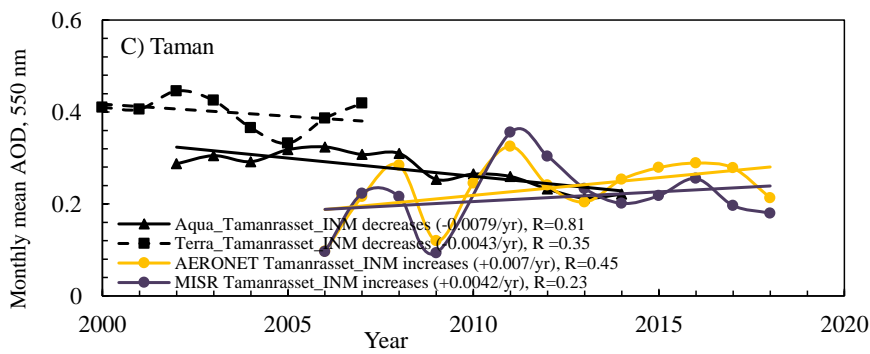
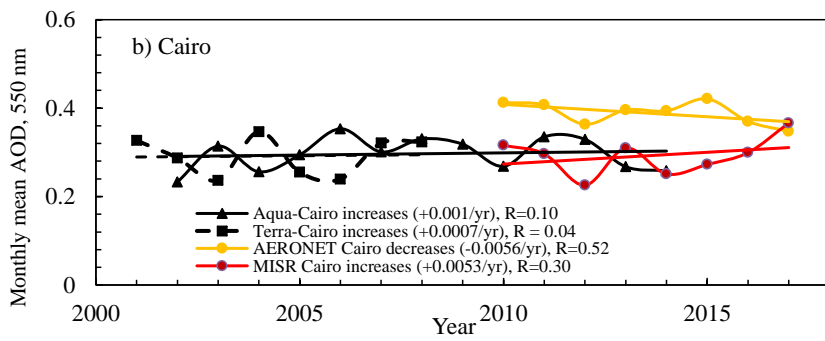
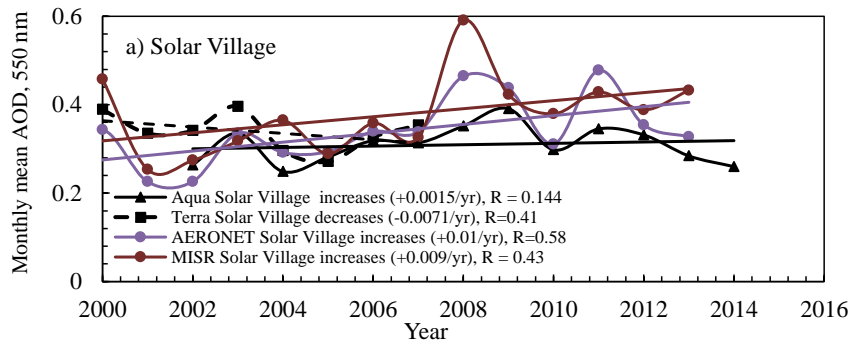
Moved up [1]: Figure 2
 Formatted: Centered, Indent: Before: 0", After: 0"
 Deleted: ¶
 <object><object>

968

Figure 3.

Deleted: ¶

Formatted: Indent: Before: 1.63", After: 0.69"



975

976

977

978

979

Figure 4.

Deleted: <object><object>

Formatted: Centered

Deleted: ¶

982
983
984
985

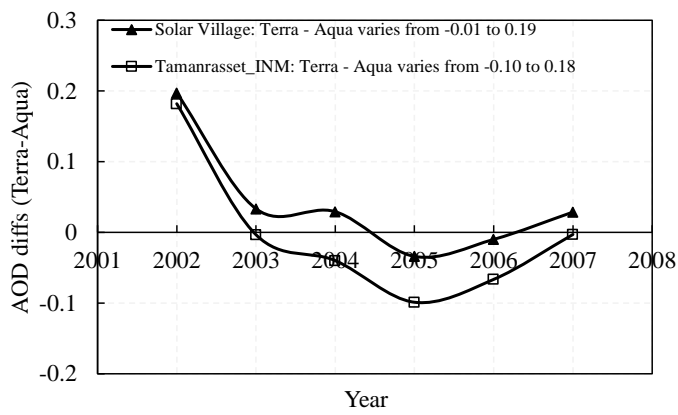
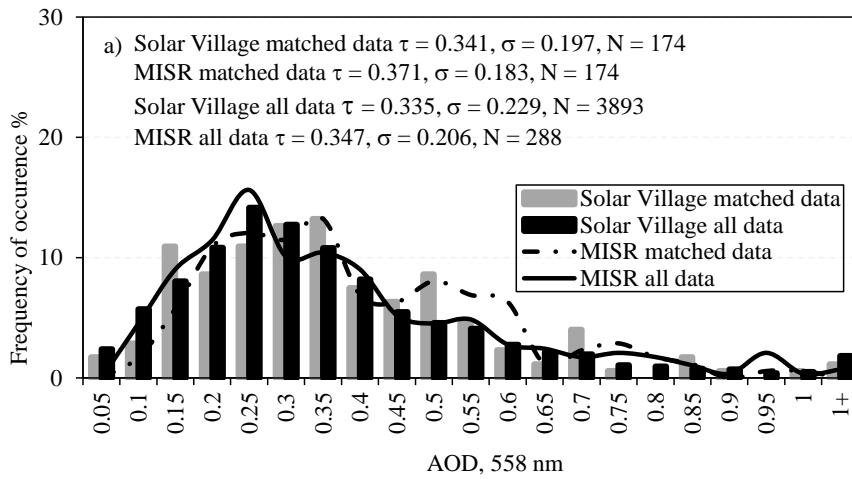


Figure 5.

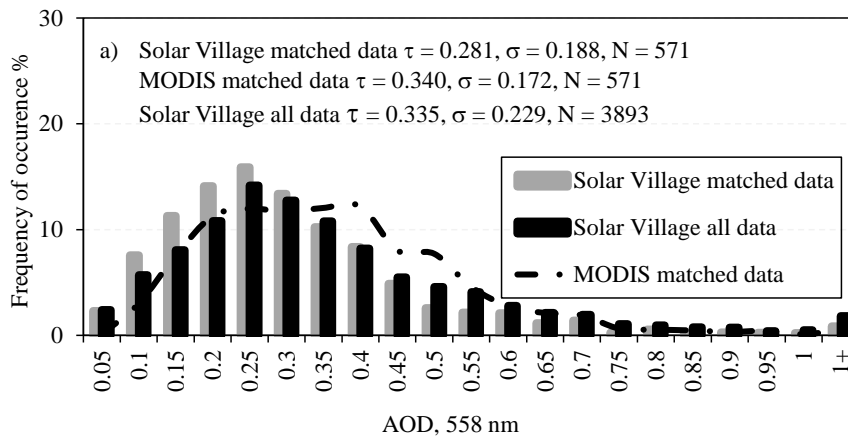
994
995
996
997
998
999
1000
1001
1002
1003
1004
1005
1006

Formatted: Centered

1007
1008
1009



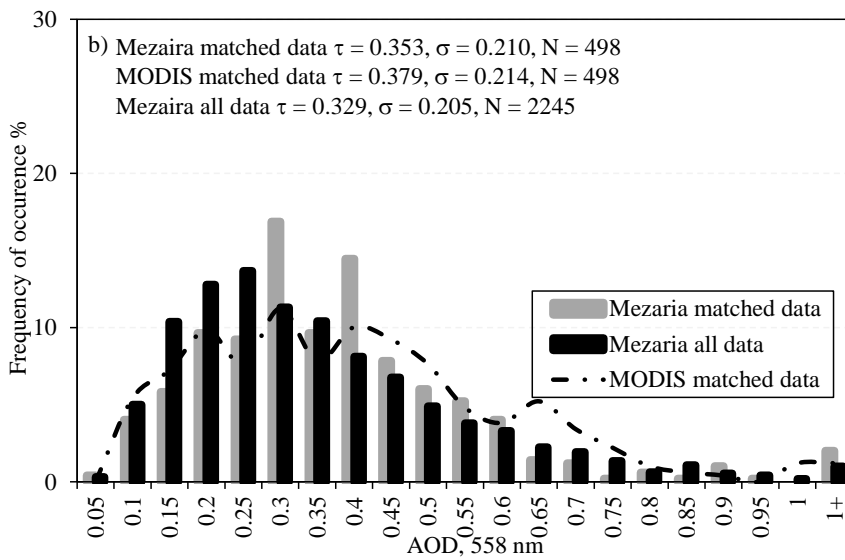
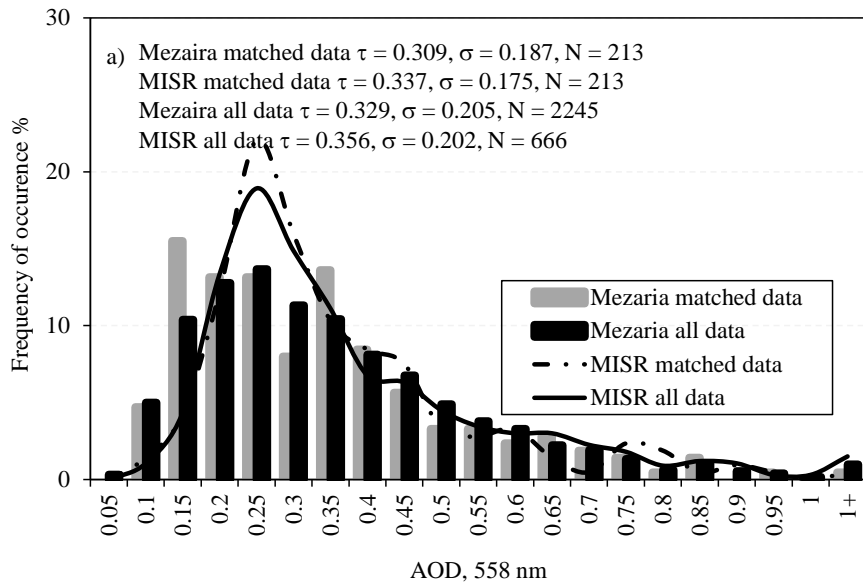
1010



1011

1012 Figure 6.

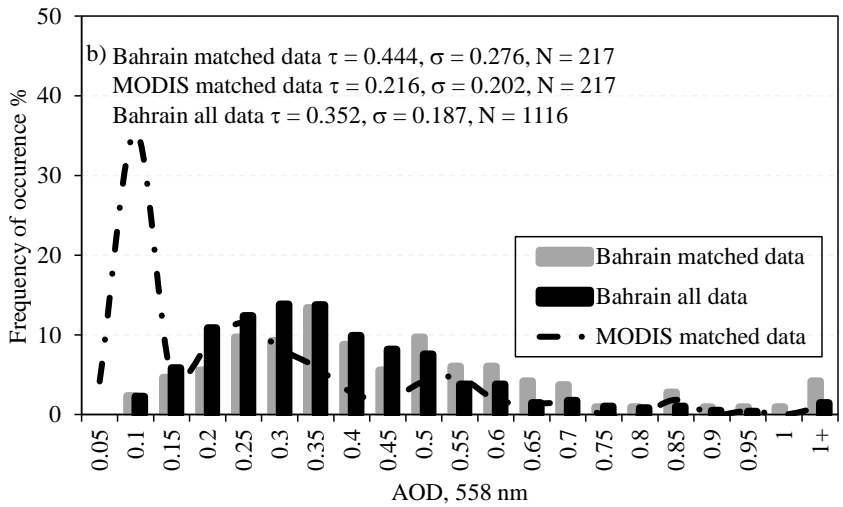
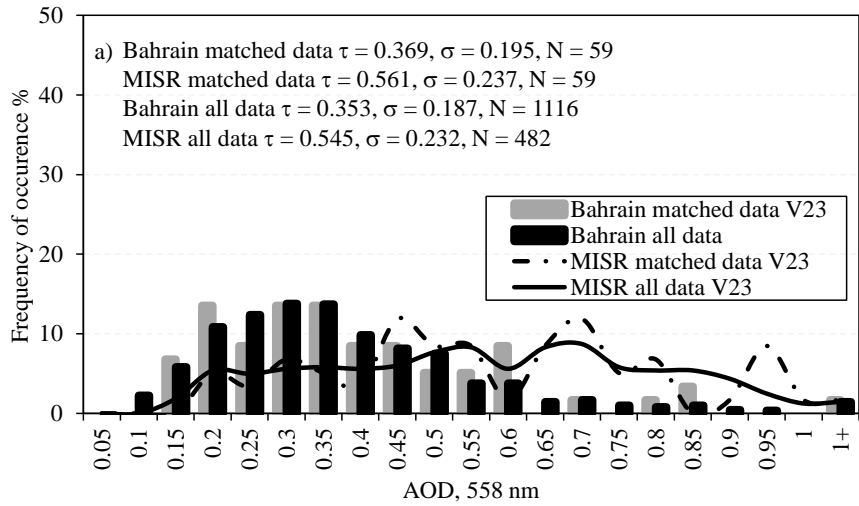
1013



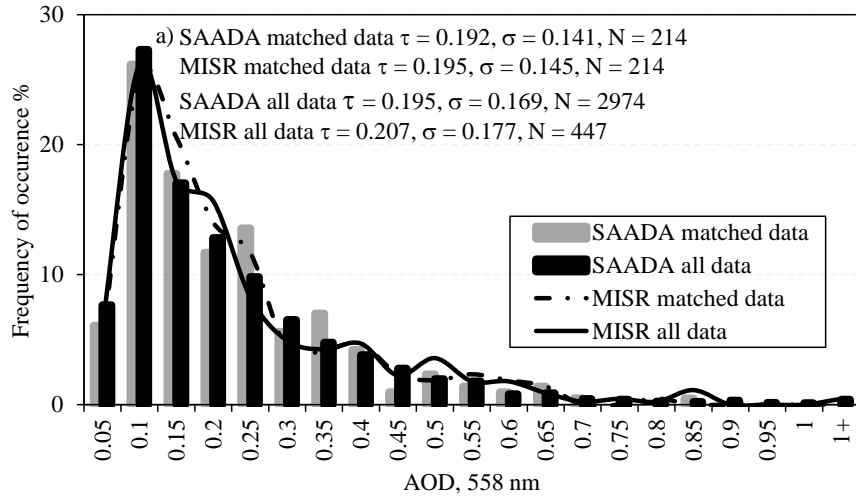
1014 Figure 7.

Deleted: ¶

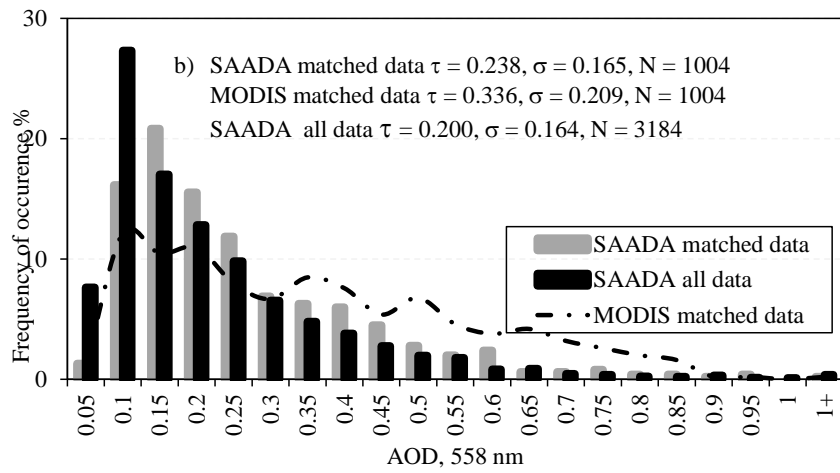
Formatted: Left



1017
 1018
 1019 Figure 8.
 1020



1021



1022

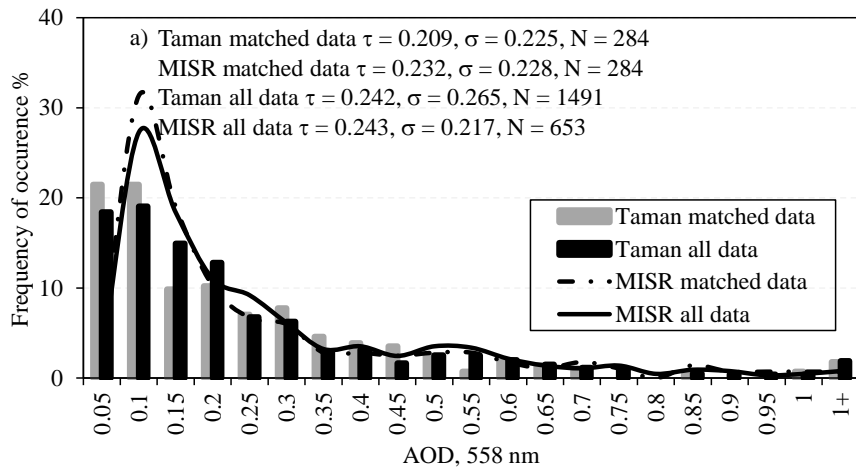
1023 Figure 9.

1024

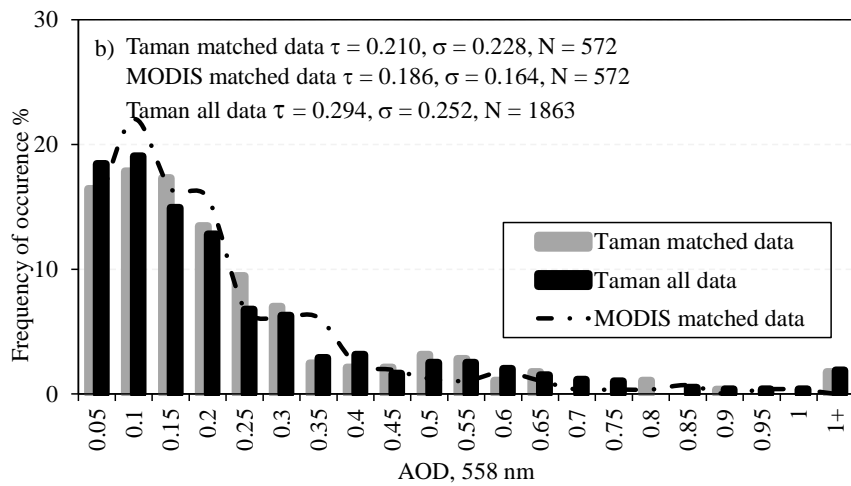
1025

1026

1027



1028



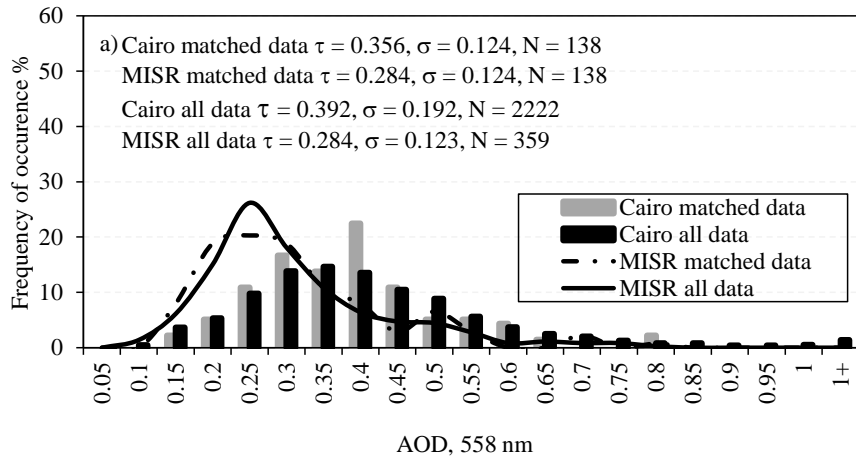
1029

1030 Figure 10.

1031

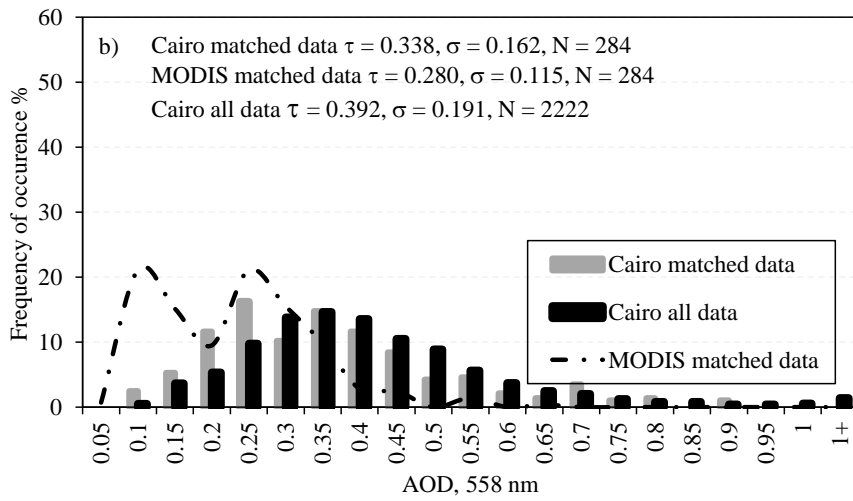
1032

1033



1034

1035

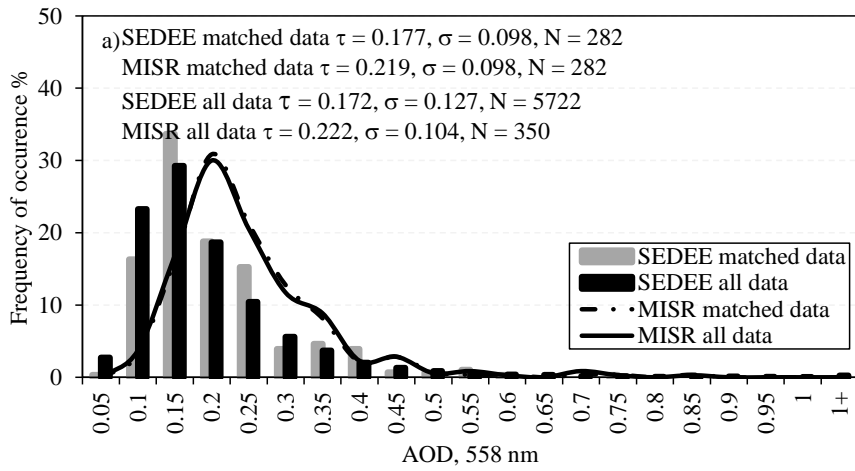


1036 Figure 11.

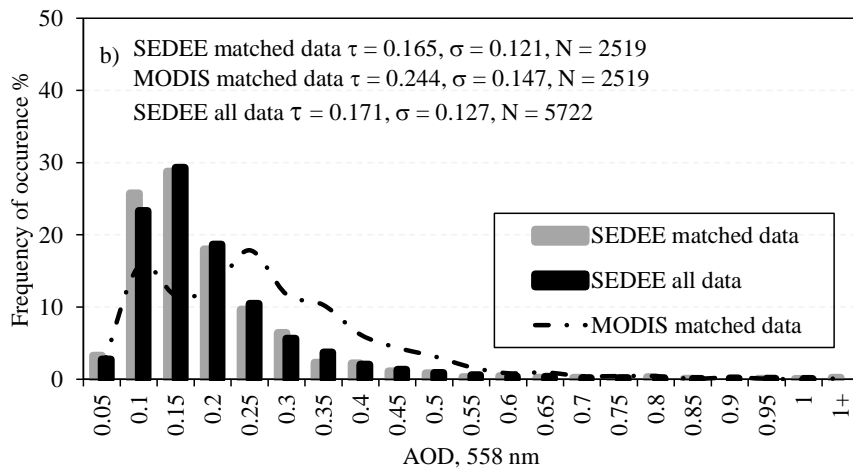
1037

1038

1039



1040



1041

1042 Figure 12.